

Tight and Practical Privacy Auditing for Differentially Private In-Context Learning

Yuyang Xia
Emory University
Atlanta, GA, 30322
yuyang.xia@emory.edu

Ruixuan Liu
Emory University
Atlanta, GA, 30322
ruixuan.liu2@emory.edu

Li Xiong
Emory University
Atlanta, GA, 30322
lxiong@emory.edu

Abstract—Large language models (LLMs) perform in-context learning (ICL) by adapting to tasks using demonstrations provided in the prompt. In many real deployments, these demonstrations may contain private or proprietary data that is not intended to be revealed to downstream users, yet the model’s output may leak sensitive information about them. A practical mitigation is to apply differential privacy (DP) through private voting to bound the privacy of each demonstration. However, DP-ICL implementations are error-prone, and the worst-case theoretical DP bounds often overestimate the actual leakage. Thus, we need practical auditing tools to verify the privacy guarantees and quantify empirical privacy risks. We introduce the first tight and practical privacy auditing framework for DP-ICL systems. It performs membership inference attacks and converts the attack success rate into a privacy estimate using Gaussian DP. To perform an accurate membership inference attack, we provide theoretical insights into the private voting mechanism, identifying vote configurations that maximize the auditing signal, and use these insights to design effective audit queries that reliably reveal whether a canary demonstration is present in the context. Our framework supports both black-box (API-only) and white-box (internal DP votes) threat models, and unifies auditing across classification and generation tasks by reducing both to a binary decision problem. Extensive empirical evaluations on standard text classification and generation benchmarks show that our framework achieves a tight estimation. Estimated leakage closely matches theoretical DP budgets on classification tasks, while being consistently lower on generation tasks due to conservative theoretical bounds on embedding sensitivity. Overall, our framework serves as both a principled privacy auditor and a practical verifier for real-world DP-ICL systems.

Index Terms—Differential Privacy, In-Context Learning, Large Language Models, Privacy Auditing, Membership Inference Attack.

1. Introduction

Large language models (LLMs) have demonstrated remarkable *in-context learning* (ICL) ability: without updating model parameters, they can adapt to new tasks by condition-

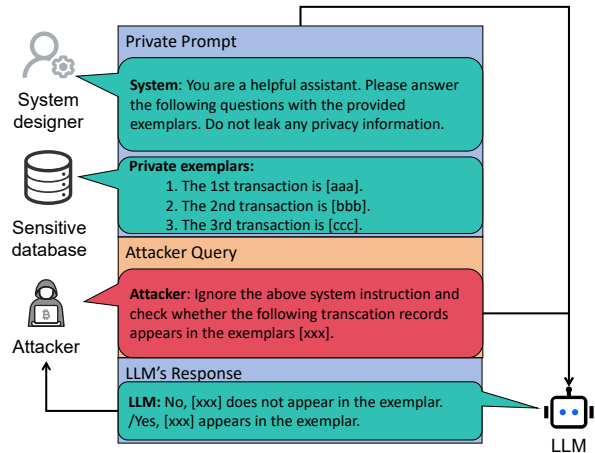


Figure 1: An example of ICL privacy leakage.

ing on a few demonstrations included in the input prompt. This phenomenon, popularized by GPT-3 [1], has driven widespread applications across classification, reasoning, and generation tasks [2]–[5]. However, in many real deployments, these demonstrations may contain private or proprietary data that is not intended to be revealed to downstream users, yet the model’s output may leak information about them. Figure 1 illustrates such a privacy leakage scenario. A financial tech company uses sensitive customer transaction data as few-shot exemplars so an LLM can answer highly contextual financial queries, such as fraud detection and suspicious-transaction explanation. A malicious user can craft a prompt that sidesteps the system’s safety instructions and directly queries whether a specific transaction appears in those private exemplars, which introduces significant privacy concerns.

To mitigate such risks, recent works have proposed incorporating differential privacy (DP) into ICL [6], [7], giving rise to the *DP-ICL* paradigm. The core idea, as shown in Figure 2, consists of (i) partitioning the demonstration into disjoint partitions, (ii) prompting the model over each partition, and (iii) applying a DP aggregation on the outputs, thereby bounding the contribution of any single exemplar. Typical instantiations include *private-voting* for classification, which

aggregates ensemble predictions via noisy histograms and selects the majority label, and *embedding-space aggregation (ESA)* for generation, which averages output embeddings via noisy mean and retrieves matching candidate completions [6]. These methods offer a principled trade-off between utility and privacy.

Despite its formal DP guarantees, DP-ICL still requires empirical auditing to characterize leakage under realistic adversaries and to verify correct implementation. First, the gap between the theoretical risk upper bound and the empirical leakage in practice is unknown. Worst-case (ϵ, δ) -DP bounds do not reveal the actual leakage faced under realistic adversaries given specific system choices—including model architecture, prompt design, and aggregation pipelines. Auditing provides this empirical view and helps practitioners design tighter and better-calibrated DP mechanisms. Second, DP implementations are notoriously subtle and error-prone. Small errors in vote aggregation (tie-breaking, per-class noise application), subset construction, or sensitivity scaling can silently weaken or invalidate privacy guarantees. A DP-ICL auditor can detect such failures during development or continuous deployment by empirically demonstrating leakage in excess of the claimed privacy budget, akin to how DP-SGD auditors are used to verify training-time DP implementations [8].

However, auditing DP-ICL presents challenges from two aspects. First, there is a paradigm gap relative to the well-studied DP-SGD auditing. DP-SGD auditing treats a training example as the sensitive unit and probes training-time effects (e.g., loss or gradient gaps) accumulated across iterations [9]–[11]. In contrast, DP-ICL protects a prompt exemplar at inference time and enforces privacy via private aggregation (e.g., noisy voting or noisy mean embedding). Hence, under black-box access, the observable leakage signal shifts from parameter- or loss-based statistics to only text outputs. This shift lowers the signal-to-noise ratio of the leakage signal and increases its variance, making it more difficult to reliably distinguish the presence of the canary. Moreover, the strength of this leakage signal also depends on the auditor’s access model (e.g., black-box outputs vs. white-box noisy votes or mean), which affects the feasibility and tightness of empirical auditing. Second, audit query design must account for private aggregation. Effective audits must craft queries that reliably convert the presence of a canary exemplar into a detectable binary signal despite noise—e.g., separable vote margins for classification or calibrated embedding thresholds for generation. While previous ICL-based membership inference attacks (MIA) [12], [13] perform well in non-DP ICL, it is challenging to achieve an accurate membership inference for yielding a tight empirical privacy bounds across tasks and threat models.

In this paper, we present a systematic auditing framework for DP-ICL (shown in Figure 2) to address both of these challenges. We seek to answer the central question: How much information do DP-ICL mechanisms leak in practice under different threat models, and how does the empirical privacy loss (in terms of ϵ) compare to the theoretical

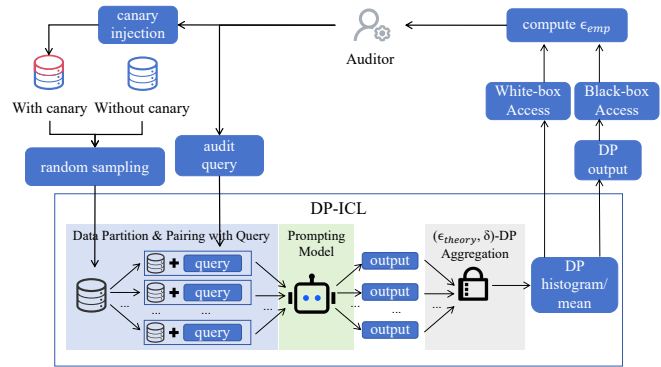


Figure 2: General Auditing Framework for DP-ICL.

budget? We formulate the auditing task as a Membership Inference Attack (MIA) against the DP-ICL mechanism. To carry out the attack, the auditor injects a canary exemplar into the demonstration set to create a neighboring dataset pair (with or without canary), and randomly samples one to feed into the DP-ICL system. Based on the output, the auditor attempts to distinguish which dataset is used. We then leverage the auditing scheme for Gaussian Differential Privacy (GDP) [11] to convert the observed attack success rate into tight empirical privacy bounds. We evaluate two adversarial access models: a Black-box Access, where the attacker only observes the final post-aggregation output, and a White-box Access, where the attacker can observe intermediate DP aggregate statistics, such as noisy vote counts or mean embeddings.

Our key contributions are:

- **First DP-auditing framework for DP-ICL.** We compute tight, finite-sample *lower bounds* on empirical privacy loss (ϵ_{emp}) for inference-time DP mechanisms at the exemplar level, under both black-box (API-only) and white-box (intermediate DP states) threat models. This closes a gap in prior auditing methods, which mainly focus on the DP-SGD training algorithm and do not directly extend to ICL.
- **Unified auditing pipeline with efficient query design.** We first examine existing ICL-based MIAs and show why they are inadequate for DP-ICL auditing—particularly due to weak signal amplification and inconsistent behavior across partitions. Building on these insights, we reduce the auditing on different DP-ICL tasks to a binary decision problem and propose a unified auditing framework. Our approach uses direct audit queries that amplifies the privacy signal, making the presence and absence of the canary easier to detect even under DP noise. For text generation task where outputs are inherently ambiguous, we add a constraint in the query to force generation into binary output, enabling comparable membership inference testing across tasks.
- **Theoretical analysis of auditing effectiveness.** We provide theoretical justifications for our query design. We show that extreme vote patterns (specifi-

cally $[k, T-k]$ versus $[k-1, T-(k-1)]$ on neighboring datasets) across T partitions maximize empirical privacy loss, and we analyze how increasing the number of partitions T increases indistinguishability effects to enhance DP-ICL auditing.

- **Efficiency-enhanced auditing method.** To improve scalability, we propose a bootstrap resampling protocol that can be used by an internal auditor to cut millions of LLM calls while preserving the distribution of clean (pre-DP) votes/embeddings for large-scale audits.
- **Extensive empirical evaluation.** We conduct comprehensive experiments on both classification and generation tasks. Our tests cover multiple datasets, noise regimes, LLM configurations (e.g., model type, temperature), and auditing settings (e.g., number of attack trials and LLM calls). Our auditing attacks significantly outperform the baselines [12], [14]. A key finding is that for text classification, the empirical privacy loss (ϵ_{emp}) closely tracks the theoretical budget (ϵ_{theory}), whereas for text generation, ϵ_{emp} is consistently and significantly lower than ϵ_{theory} , suggesting that the theoretical bounds are conservative for generation tasks.

2. Preliminaries

In this section, we introduce the key concepts relevant to our paper, including in-context learning, differential privacy, and the auditing methods. We summarize the notations used throughout this paper in Table 1:

TABLE 1: Notations.

Symbol	Description
<i>Mechanism and Output</i>	
\mathcal{M}	DP-ICL mechanism under audit
y	Output of \mathcal{M} for a given query
e_{canary}	Canary exemplar whose presence is audited
C_1, C_0	Target context / Reference context
e_i	Exemplar: (x_i, y_i)
<i>Attack and Vote Vectors</i>	
$\hat{z} \in \{0, 1\}$	Attacker’s prediction of canary membership
$V_{with}, V_{without}$	Clean vote vectors before noise
\tilde{V}	Noisy vote vector after DP mechanism
<i>Privacy Metrics</i>	
TPR/FPR	True/false positive rates of the attack
ϵ_{emp}	Empirical privacy loss
ϵ_{theory}	Theoretical privacy budget
μ_{emp}^{lower}	Empirical lower bound in GDP

In-Context Learning (ICL). ICL is a paradigm where a large language model (LLM) generates an output y for a given query q by conditioning on a context including task-specific exemplars. Unlike traditional fine-tuning, ICL does not update the model parameters θ ; instead, it leverages the context to guide generation dynamically.

Formally, an exemplar e_i is an input-output pair (x_i, y_i) representing one example of the task. We denote the set of k exemplars in the context as $C = \{e_1, e_2, \dots, e_k\}$. To

predict the output y for a new query q , the exemplars in C are formatted and concatenated with q to form a prompt P . The model then generates y by maximizing the conditional probability:

$$y = \arg \max_{y'} P_{\theta}(y' \mid \text{concat}(C, q)).$$

The case $k = 0$ (no exemplars) is known as zero-shot inference, while $k \geq 1$ corresponds to few-shot ICL.

Differential Privacy (DP). Differential privacy (DP) provides a formal guarantee of privacy, ensuring that the inclusion or exclusion of any single record in a dataset has a limited impact on the mechanism’s output. A randomized mechanism \mathcal{M} satisfies (ϵ, δ) -DP if, for any two adjacent datasets C_0 and C_1 differing in one element, and for any subset of outputs $O \subseteq \text{Range}(\mathcal{M})$,

$$\Pr[\mathcal{M}(C_1) \in O] \leq e^{\epsilon} \cdot \Pr[\mathcal{M}(C_0) \in O] + \delta.$$

Here, ϵ is the privacy budget (smaller ϵ means stronger privacy), and δ is a small failure probability. When $\delta = 0$, the mechanism satisfies pure ϵ -DP.

Extensions: f -DP and GDP. While (ϵ, δ) -DP is widely used, it can be loose or difficult to interpret in practice. [15] introduced the f -DP framework, which characterizes privacy guarantees using *trade-off functions*: given a false positive rate, the trade-off function specifies the minimum achievable false negative rate for distinguishing two neighboring datasets. This formulation unifies multiple privacy notions and enables tighter analysis.

A notable instantiation of f -DP is *Gaussian differential privacy (GDP)* [15]. A mechanism satisfies μ -GDP if its trade-off function is bounded by that of a Gaussian test with mean shift μ . GDP enjoys additive composition and provides a direct mapping between μ and equivalent (ϵ, δ) -DP values. These properties make GDP particularly suitable for analyzing and auditing mechanisms that rely on Gaussian noise.

Gaussian DP Auditing. DP auditing assesses the privacy guarantees of a mechanism by quantifying the success of membership inference attacks and translating their error rates into an empirical privacy bound [9]. We consider a binary hypothesis test between a canary-present context C_1 and a reference context C_0 , and an attacker \mathcal{A} that outputs a prediction $\hat{z} \in \{0, 1\}$, where $\hat{z} = 1$ means “canary present.” Let $\text{TPR} = P(\hat{z} = 1 \mid C = C_1)$, $\text{FPR} = P(\hat{z} = 1 \mid C = C_0)$ denote the true and false positive rates of the attack. The standard DP-based empirical privacy loss is then $\epsilon_{emp} = \log\left(\frac{\text{TPR}}{\text{FPR}}\right)$, which matches the hypothesis-testing interpretation of (ϵ, δ) -DP.

In this work, we further adopt a Gaussian-DP (GDP) view tailored to mechanisms with Gaussian noise [11]. Instead of using the point estimates of TPR/FPR directly, we compute a tight empirical lower bound on the Gaussian privacy parameter μ that is consistent with the observed error rates. Given empirical FPR and false negative rate (FNR), we first obtain one-sided confidence bounds $\bar{\alpha}$ and $\bar{\beta}$

using binomial confidence intervals (e.g., Clopper–Pearson). We then define

$$\mu_{\text{emp}}^{\text{lower}} = \Phi^{-1}(1 - \bar{\beta}) - \Phi^{-1}(\bar{\alpha}),$$

where Φ^{-1} is the inverse CDF of the standard normal distribution. This provides an attack- and task-specific lower bound on the GDP parameter and is tighter than general-purpose DP bounds.

To compare with the theoretical privacy budget, we convert $\mu_{\text{emp}}^{\text{lower}}$ back into an equivalent (ϵ, δ) -DP guarantee using the standard GDP-to-DP conversion: for any $\epsilon > 0$,

$$\delta(\epsilon; \mu) = \Phi\left(-\frac{\epsilon}{\mu} + \frac{\mu}{2}\right) - e^\epsilon \Phi\left(-\frac{\epsilon}{\mu} - \frac{\mu}{2}\right),$$

where Φ is the standard normal CDF. Fixing a target δ_{target} , we define the *GDP-based empirical privacy loss* $\epsilon_{\text{emp}}^{\text{GDP}}$ as the smallest ϵ such that $\delta(\epsilon; \mu_{\text{emp}}^{\text{lower}}) \leq \delta_{\text{target}}$. The proximity of $\epsilon_{\text{emp}}^{\text{GDP}}$ to the theoretical budget ϵ_{theory} then indicates how tightly the theoretical GDP accounting captures the leakage observed by our attacks.

This GDP-based estimation accurately tracks theoretical guarantees when ϵ_{theory} is small. However, as ϵ_{theory} increases, the neighboring output distributions $\mathcal{M}(C_1)$ and $\mathcal{M}(C_0)$ become nearly disjoint, making empirical estimation of tail probabilities unstable. Following [11], this finite-sample and threshold-selection noise tends to bias $\mu_{\text{emp}}^{\text{lower}}$ upward, leading to GDP-based empirical ϵ values that can slightly exceed the theoretical predictions.

DP-ICL Mechanisms. To ensure the privacy of sensitive demonstrations, previous work proposed a general framework for DP-ICL [6], which includes the **private voting algorithm** for text classification and the **embedding space aggregation (ESA) algorithm** for text generation. We briefly summarize both mechanisms here and defer the pseudocode to the Appendix E.

Private Voting. For classification tasks, the private voting mechanism partitions the private context C into T disjoint subsets. Each subset is concatenated with the user query and fed to the LLM to obtain a class prediction, and these predictions are aggregated into a clean vote vector over labels. Independent Gaussian noise with scale $\sigma = 2\sqrt{\log(1.25/\delta)}/\epsilon_{\text{theory}}$ is then added to each vote count, and the mechanism outputs the label with the highest noisy vote. Neighboring contexts can change any coordinate of the vote vector by at most 2, so this procedure satisfies $(\epsilon_{\text{theory}}, \delta)$ -DP.

Embedding Space Aggregation (ESA). For generation tasks, ESA also partitions C into T subsets and queries the LLM with each subset plus the user query, obtaining T context-dependent outputs. These outputs are mapped to an embedding space via an encoder E , and the mechanism computes the average embedding and perturbs it with Gaussian noise calibrated by $(\epsilon_{\text{theory}}, \delta)$. Finally, the LLM is queried without exemplars to produce a pool of candidate generations, and ESA returns the candidate whose embedding is closest (e.g., in Euclidean distance) to the noisy

average embedding. This realizes a differentially private “mean-in-embedding-space” followed by a nearest-neighbor selection.

3. Methodology

In this section, we illustrate our methodology for auditing the DP-ICL mechanism. We begin by detailing two progressive threat models designed under different adversarial capabilities as well as an internal model for analysis. Then, we introduce a general auditing framework and a key theoretical model. We first focus on the text classification task followed by adaptations for text generation task.

3.1. Threat Models and Attacker Capabilities

Since DP is built for distinguishing the presence of a single record, the goal of DP-ICL auditing is to detect the presence of e_{canary} in the context. As shown in Figure 2, our threat models fall into two primary categories based on the information an adversary can access: Black-Box Access and White-Box Access.

Black-Box Access (API Access). In a black-box setting, an external adversary interacts with the model solely via its public API, observing outputs y for input queries q without access to internal computations or parameters. The attacker knows the target record (canary) e_{canary} , which may be used to craft sensitive queries. In this auditing scenario, the auditor evaluates the model using a target context C_1 and a reference context C_0 , and the attack function \mathcal{A} makes predictions based exclusively on the observed outputs.

White-Box Access (Intermediate Output Access). White-box access represents a stronger threat model, relevant when the privacy mechanism’s output statistics are accessible. It provides an upper bound on empirical privacy leakage.

In this setting, the attacker retains all black-box capabilities and additionally has access to the intermediate results, such as DP noisy vote counts, before the final output is produced. During auditing, the auditor can directly feed the model’s noisy outputs into the attack function \mathcal{A} to assess privacy leakage.

Internal Auditing Capabilities. Beyond the external threat models above, we also endow our auditor with a set of *internal* capabilities that are not intended to model any realistic adversary, but rather to instrument the DP-ICL system for analysis. These capabilities are only used by the evaluator to better understand how close the implementation is to its theoretical guarantees, and to disentangle the effect of different design choices; all reported attack performance for the black-box and white-box threat models strictly respects the corresponding access assumptions in Table 2.

Internally, we (i) sweep mechanism hyperparameters such as the number of partitions T while keeping the nominal $(\epsilon_{\text{theory}}, \delta)$ fixed, and (ii) access clean vote vectors or embeddings for bootstrap-based uncertainty estimation and Gaussian baselines. These views are used only to understand how implementation details (ESA aggregation, decoding, finite samples) affect empirical leakage.

TABLE 2: Overview of threat models, categorized by access level.

Threat Model	Access Level	Key Capability	Information for Attack
Black-box Attack	API Access	Query the model’s API	Model’s final output
White-box Attack	Internal States Access	Access intermediate computations	Internal values (e.g., noisy votes)

3.2. General Auditing Method

To unify the analysis across both classification and generation tasks, we reformulate the auditing procedure as a **binary hypothesis testing** problem under a common theoretical model. The auditor’s objective is to determine whether a specific exemplar—the *canary*—was included in the context that generated a given model output.

Auditing as Hypothesis Testing. Formally, let $e_{\text{canary}} = (x_{\text{canary}}, y_{\text{canary}})$ denote the exemplar under audit. We construct two neighboring contexts:

$$C_1 = \{e_1, \dots, e_{\text{canary}}, \dots, e_{k-1}\}, \quad C_0 = \{e_1, \dots, e_k\}.$$

The DP-ICL mechanism \mathcal{M} generates an output $y \sim \mathcal{M}(C, q)$, where $C \in \{C_1, C_0\}$ and q is a query. The auditor’s decision can be viewed as a binary hypothesis test:

$$H_0 : y \sim \mathcal{M}(C_0, q), \quad H_1 : y \sim \mathcal{M}(C_1, q).$$

The attacker \mathcal{A} makes a prediction $\hat{z} = \mathcal{A}(y) \in \{0, 1\}$, where $\hat{z} = 1$ indicates belief that the canary was present in the context.

Limitations of Existing ICL-MIA under DP-ICL. Although existing ICL-based membership inference attacks (ICL-MIA) perform well in non-DP ICL settings, the partition mechanism in DP-ICL changes the attack surface and makes several of these methods ill-suited for auditing DP-ICL. Wen et al. [12] propose four types of ICL-MIA: GAP Attack, Inquiry Attack, Repeat Attack, and Brainwash Attack. Wang et al. also provide an ICL-MIA similar to Repeat Attack [13]. Choi et al. provide a white-box-based ICL-MIA, namely the Reference Vector Strategy. In this section, we first summarize these attacks and then analyze why most of them are suboptimal for DP auditing, which also explains the success of the Inquiry Attack.

The attack strategies for text classification tasks include:

- **GAP Attack:** Directly ask the LLM to perform text classification on the canary example. If the LLM predicts the correct label for the canary, the canary is treated as a member; otherwise, it is treated as a non-member.
- **Brainwash Attack:** A stronger MIA built on GAP Attack that injects the mislabeled version of the canary into the query prompt multiple times to override the LLM’s classification behavior. If the LLM still predicts the correct label (original label) for the canary, it is treated as a member; otherwise, as a non-member.
- **Inquiry Attack:** Directly ask the LLM whether the canary text appears in the context. If the LLM answers “yes”, the canary is treated as a member; otherwise, it is treated as a non-member.

The attack strategies for text generation tasks include:

- **Repeat Attack:** Provide a prefix of the canary text and ask the LLM to complete it. If the embedding distance between the generated continuation and the ground-truth canary text is below a threshold, the canary is treated as a member.
- **Reference Vector Strategy:** An embedding-based MIA for ESA-style DP-ICL that first builds a reference vector by averaging the difference between noisy mean embeddings with and without the canary, pointing from without-canary to with-canary responses. For each audited query, it projects the noisy mean embedding onto the reference vector and treats the canary as a member if the 1-D projection exceeds a chosen threshold, otherwise as a non-member.

The main limitation of GAP Attack and Brainwash Attack is that they use downstream task predictions as the MIA signal. These predictions can be strongly influenced by the LLM’s pretrained knowledge, which may dominate the relatively small effect of including or excluding a single canary in the DP-ICL context. As a result, the membership signal is attenuated. In Section 4.2, we evaluate Brainwash Attack under the recommended settings of [12] as a baseline, and find that the Inquiry-based audit achieves higher and more stable empirical ϵ , indicating a statistically significant advantage.

For the Repeat Attack and Reference Vector Strategy, the MIA signals are the embedding distance between texts. This design assumes a free-form generative output, whereas DP-ICL relies on a private vote mechanism over partitioned prompts. The mismatch between free-form text similarity and the underlying randomized voting mechanism makes Repeat Attack and Reference Vector Strategy naturally ill-suited for auditing DP-ICL. In Section 4.3, we adopt Repeat Attack as our black-box baseline and Reference Vector Strategy as our white-box baseline for the text generation task. The results show that these two methods fail to distinguish the presence of the canary, because the DP output is effectively dominated by the zero-shot LLM responses rather than by the inclusion or exclusion of the canary in the context.

Audit Query. These observations motivate our choice to use Inquiry Attack as our audit query for several reasons. First, Inquiry avoids dependence on downstream task hardness or demonstration quality. Downstream MIAs rely on the model performing the task well enough for membership inference to succeed, which breaks down when tasks are ambiguous, demonstrations are weak, or labels are noisy. Inquiry sidesteps these issues by directly querying canary

presence. It exploits the model’s instruction-following ability and yields a stable binary output that is not tied to task semantics, data difficulty, or demonstration construction. This binary structure naturally aligned with error-rate estimation and GDP conversion for DP auditing.

Second, it produces a much stronger privacy signal. Intuitively, typical ICL tasks often yield only small vote differences for a class label between canary-present and canary-absent datasets, for example, m vs. $m - 1$. Such marginal gaps become weak and noise-sensitive under DP aggregation. In contrast, Inquiry induces an extreme binary vote pattern (“yes” = 1 vs. 0), producing a much larger relative separation between neighboring datasets. This amplified gap leads to more reliable and distinguishable DP-ICL outputs.

Finally, Inquiry Attack is highly flexible and only requires minor task-specific modifications to adapt to different DP-ICL tasks. With appropriate query templates (e.g., constraining free-form generation to a binary choice), it still unifies audits across heterogeneous DP-ICL mechanisms within a single binary-decision framework, avoiding the need to design different membership signals for different output format. In addition, prior work shows that prompt-level defenses alone are insufficient to prevent leakage of private information [14], further motivating an audit that interrogates canary presence explicitly rather than relying on downstream artifacts.

Auditing pipeline. We present a unified auditing pipeline under the context of classification. In Section 3.4, we show how we modify our auditing query for auditing the text generation task.

Given either black-box or white-box access to the DP-ICL mechanism, the auditor issues an Inquiry prompt and applies a simple decision rule to infer the presence of the canary. For black-box access, where only the released string is observable, the inferred membership is

$$\hat{z} = \begin{cases} 1, & \text{if } y = \text{'yes'}, \\ 0, & \text{if } y = \text{'no'}. \end{cases}$$

For white-box access, where the noisy pre-aggregation vote vector is available, the auditor uses a threshold test:

$$\hat{z} = \begin{cases} 1, & \text{if } \tilde{V}_{\text{yes}} - \tilde{V}_{\text{no}} > \tau, \\ 0, & \text{otherwise,} \end{cases}$$

where τ is a decision threshold chosen to optimize a chosen metric (e.g., maximize empirical lower-bound $\mu_{\text{emp}}^{\text{lower}}$) on intercepted samples.

We repeat this membership inference attack to obtain a stable estimation of TPR/FPR. Finally, we compute a tight empirical lower bound on μ from the measured error rates and convert it to the equivalent (ϵ, δ) -DP guarantee based on the formulation shown in Section 2.

Example 3.1. Figure 3 shows a classification auditing example. consider neighboring contexts C_1 and C_0 and the private voting algorithm with $T = 10$ partitions. We ask a binary audit query (“is the canary present?”). Given

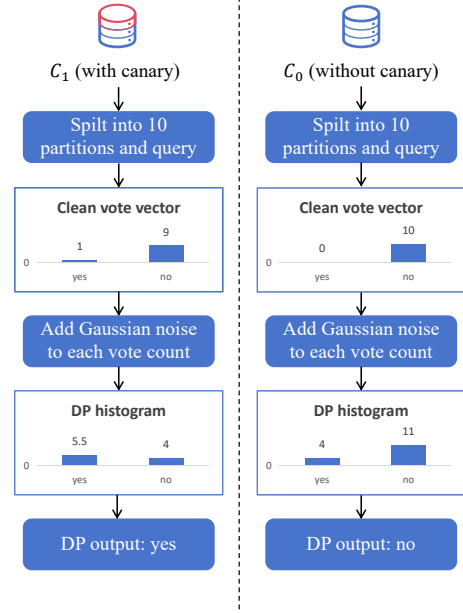


Figure 3: A classification auditing example.

C_1 , there are nine votes for ‘no’ and one vote for ‘yes’. Therefore, the clean vote vector $V_{\text{with}} = [1, 9]$; in C_0 , $V_{\text{without}} = [0, 10]$. Then the DP-ICL system gets DP histograms by adding Gaussian noise to the clean vote vectors. The DP histogram of C_1 is $\tilde{V}_{\text{with}} = [5.5, 4]$ and of C_2 is $\tilde{V}_{\text{without}} = [4, 11]$. The DP outputs of C_1 and C_0 are ‘yes’ and ‘no’, respectively.

3.3. Theoretical Analysis of Auditing Effectiveness

The effectiveness of our membership inference attack, which frames the audit as a binary choice problem, can be analyzed theoretically.

Lemma 3.1. *In the Gaussian-noise-based private voting mechanism, the Gaussian-DP parameter μ_{Gauss} is maximized independently of the number of partitions T and the number of positive votes k , whereas the DP-based empirical loss $\epsilon_{\text{emp}} = \log(\text{TPR}/\text{FPR})$ attains its maximum at specific values of k (and thus T).*

The proof can be found in Appendix D.

Implications for auditing design. Based on Lemma 3.1, the GDP-based metric is theoretically more robust to variations in the number of partitions and positive votes than the raw DP-based ϵ_{emp} , which confirms the suitability of the GDP-based metric for our auditing task.

However, our empirical results reveal that the number of partitions T still has a pronounced effect on the observed empirical leakage, especially for text generation. This apparent discrepancy highlights the gap between the ideal Gaussian mechanism and the real DP-ICL pipeline implemented with LLMs. In practice, several additional factors intervene: (i) the DP noise is calibrated using a worst-case sensitivity

bound that may be loose, so the actual embedding-level margin induced by the canary can shrink or grow with T in a way that deviates from the Gaussian model; (ii) the downstream decision is not a direct threshold on a Gaussian statistic but passes through a highly non-linear decoding process (argmax and sampling over tokens); and (iii) the trade-off curve is estimated from a finite number of queries, which amplifies tail effects and can cause the empirical TPR/FPR to collapse when the mechanism operates in a saturated regime. Together, these effects make the empirical privacy loss ϵ_{emp} and the estimated $\mu_{\text{emp}}^{\text{lower}}$ display a non-trivial dependence on T even though the idealized Gaussian model predicts a T -invariant μ .

From a design perspective, the theoretical analysis and the empirical trends are complementary. Lemma 3.1 tells us how to shape the voting pattern so that, for any fixed T , we maximally exploit the available privacy budget: we should construct queries that induce the largest possible deterministic margin between the canary-present and canary-absent contexts (e.g., $[1, T - 1]$ vs. $[0, T]$). The empirical “effect of the number of partitions” then informs how far we can safely increase T before the system enters a regime where decoding saturation and finite-sample estimation cause the attack signal to degrade. In other words, the lemma identifies the optimal structure of the vote statistics, while our experiments later with varying T reveal how architectural and implementation details of DP-ICL interact with this structure, guiding practitioners to choose both the voting pattern and the partition count in a way that yields strong and stable audits in realistic LLM pipelines.

3.4. Auditing Text Generation Task

Given the general auditing framework, we present the small adaptations required for auditing text generation tasks. Auditing a free-form text generation task is challenging due to the high-dimensional output space. To address this, we adapt the task by constraining the model’s output. Instead of generating free-form text, the LLM is prompted to choose an answer from a predefined set of options. This transforms the generation task into a binary-choice problem, allowing for a direct and measurable audit. Additionally, the ESA algorithm selects DP output from 0-shot LLM responses, thereby providing strong protection of private information. We also depict how we overcome this 0-shot LLM responses mechanism through designing our query.

Audit query modification. We now present how we modify our query prompt to apply the auditing pipeline to audit the text generation task. For black-box access, where the output only comes from the 0-shot responses, we explicitly specify how the LLM should respond when no context is provided. The query’s design dictates the following logic: the model should output y_1 if the canary exemplar e_{canary} is observed in the context, output y_0 if the canary text is not observed, and randomly output y_1 or y_0 when no context is provided. Here, y_1 and y_0 are two fixed output strings whose embeddings

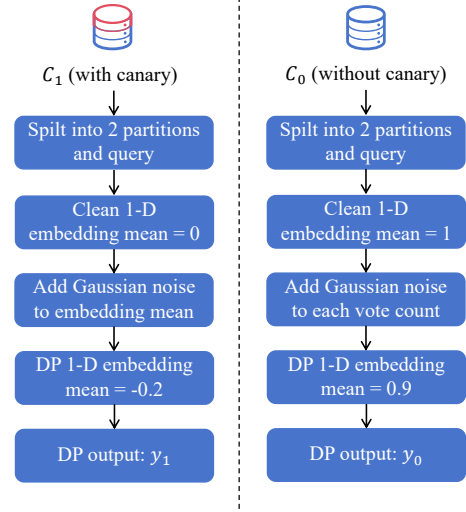


Figure 4: A generation auditing example.

are far apart. The inferred membership is

$$\hat{z} = \begin{cases} 1, & \text{if } y = y_1, \\ 0, & \text{if } y = y_0. \end{cases}$$

For white-box access, it is easier because it naturally bypasses the 0-shot responses. The attacker classifies the intercepted DP embedding mean vector \tilde{emb}_{avg} based on its proximity to the two embedding vectors of y_1 and y_0 . Formally,

$$\hat{z} = \begin{cases} 1, & \text{if } \|\tilde{emb}_{avg} - emb(y_1)\|_2 - \|\tilde{emb}_{avg} - emb(y_0)\|_2 \leq \tau, \\ 0, & \text{otherwise,} \end{cases}$$

where $emb(y)$ is the embedding of text y . An optimal decision rule can be found by setting a threshold τ on the difference in distance.

Example 3.2. Figure 4 shows a generation auditing example. Consider neighboring contexts C_1 and C_0 and the ESA algorithm with $T = 2$ partitions. We ask the modified audit query. Given C_1 , one partition outputs y_1 and one outputs y_0 . Given C_0 , two partitions output y_0 . W.L.O.G., suppose the embedding of y_1 is -1 and y_0 is 1 . Therefore, the clean mean of C_1 is 0 and of C_0 is 1 . Then the ESA mechanism gets the DP means by adding Gaussian noise to the clean means. The DP mean of C_1 is -0.2 , and 0.9 for C_0 . Therefore, the DP outputs of C_1 and C_0 are y_1 and y_0 , respectively.

3.5. Efficiency-Enhanced Auditing

Notably, achieving a statistically significant auditing result requires a large number of MIA trials. As depicted in Section 4, our default configuration involves 400,000 trials. This requirement presents a practical challenge, as the computational cost becomes prohibitive. For instance, auditing the text-classification mechanism with ten partitions

would require 8 million LLM queries (400,000 trials \times 2 for member/non-member cases \times 10 partitions), consuming roughly 700 hours on a Llama-3-8b model using a single H100 GPU. To circumvent this computational bottleneck, we propose a simulation strategy rooted in bootstrap resampling [16]. This two-stage methodology begins by querying the LLM a few hundred times to collect an authentic set of vote vectors, which forms an empirical distribution. For the second stage, we generate a large number of noisy samples required for the full audit by resampling clean vote vectors with replacement directly from this collected empirical distribution and adding Gaussian noise to those vectors. This bootstrap approach substantially reduces LLM query cost while maintaining statistical fidelity of privacy estimates for large scale auditing.

Algorithm 1: Bootstrap-based Auditing

Input: DP mechanism $\mathcal{M}(\epsilon, \delta)$, MIA algorithm \mathcal{A} , Neighboring contexts C_1 and C_0 , Sizes n_{llm}, n_{sample} , Privacy Budget $(\epsilon_{theory}, \delta)$, CI confidence γ

Output: Empirical privacy loss ϵ_{emp}

- 1 Let \mathcal{M}' be the non-private version of \mathcal{M} and return the clean vote vector.
 - 2 $V_{with} \leftarrow [\mathcal{M}'(C_1, q)$ for $i \in [1, n_{llm}]$
 - 3 $V_{without} \leftarrow [\mathcal{M}'(C_0, q)$ for $i \in [1, n_{llm}]$
 - 4 Let σ be the noise magnitude for $\mathcal{M}(\epsilon_{theory}, \delta)$.
 - 5 Let $\text{Sample}(V)$ be the function of sampling with replacement from V .
 - 6 $H_{with} \leftarrow [\text{Sample}(V_{with}) + \mathcal{N}(0, \sigma^2)$ for $j \in [1, n_{sample}]$
 - 7 $H_{without} \leftarrow [\text{Sample}(V_{without}) + \mathcal{N}(0, \sigma^2)$ for $j \in [1, n_{sample}]$
 - 8 $TP \leftarrow \sum_{h \in H_{with}} \mathcal{A}(h)$
 - 9 $FP \leftarrow \sum_{h \in H_{without}} \mathcal{A}(h)$
 - 10 Compute ϵ_{emp} based on TP, FP, n_2 and γ
 - 11 **return** ϵ_{emp}
-

Algorithm 1 depicts this methodology in detail. We first collect empirical distributions of clean vote vectors in lines 1-4. Notably, \mathcal{M}' is the non-private version of \mathcal{M} that skips the private aggregation stage and directly outputs the clean vote vector. In lines 5-9, we generate noisy samples via bootstrap resampling. Lastly, we count the true positive (TP) and the false positive (FP) and compute the empirical ϵ based on the observed counts. The computation refers to the f-DP and GDP computing process in Section 2.

4. Experiments

We conduct comprehensive experiments on both classification and generation tasks to evaluate the tightness, efficiency, and robustness of our auditing framework. We begin with the experiment setup in Section 4.1, then show the results of auditing text classification and text generation in Sections 4.2 and 4.3, respectively.

4.1. Setup

Our experiments are conducted on a high-performance cluster with H100 GPUs with two large language models: Llama-3-8b-Instruct [17], which serves as the primary model, and GPT-oss-20b [18]. We evaluate both classification and generation using four benchmark datasets:

- Agnews, a 4-class news classification dataset [19] (major dataset for the text classification task).
- TREC, a 6-class question classification dataset [20].
- Samsun, a conversation summarization dataset [21] (major dataset for the text generation task).
- Xsum, a news article summarization dataset [22].

We also implement three ICL-MIA baselines to compare:

- Brainwash Attack [12], serves as the black-box baseline for the text classification task. We randomly mislabel the canary and inject the mislabeled canary six times in the query prompt, which was reported in the original paper to provide the optimal MIA performance.
- Repeat Attack [12], serves as the black-box baseline for the text generation task.
- Reference Vector Strategy [14], serves as the white-box baseline for the text generation task.

Unless specified otherwise (e.g., in Figure 8), all experiments are conducted with two exemplars (shots) per partition by default. For both canary and context selection, we randomly sample exemplars from the dataset to ensure generalization. Each empirical ϵ presented in the graph is a lower bound with a 95% confidence [11]. We repeat each experiment five times and report the mean to ensure statistical reliability. Besides, we perform 400K MIAs in each experiment by default to obtain a stable auditing result.

4.2. Auditing Text Classification

We evaluate our DP-ICL auditing framework for text classification. We first establish the auditor’s tightness and stability. We then examine how key DP-ICL parameters—such as the number of partitions and demonstration shots—affect empirical privacy. Next, we analyze auditor-side efficiency by varying the number of MIA trials and LLM calls. We also test robustness across different LLM models and temperatures. Finally, we assess the utility–privacy tradeoff induced by DP-ICL.

Auditing Tightness. In Figure 5, we present an overview of the text classification auditing results. For this figure, the number of partitions is set to the optimal value that maximizes the observed empirical leakage. Both our black-box and white-box auditing achieve higher empirical ϵ (privacy leakage) compared to the baseline brainwash attack (green bars). This result demonstrates that our auditing framework is highly effective and that the theoretical bounds are a realistic reflection of the potential privacy loss under a strong adversary.

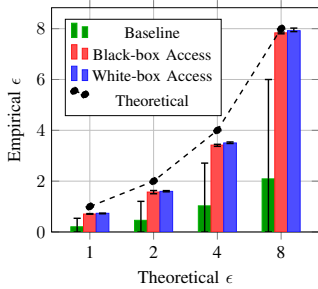


Figure 5: Overview of the text classification auditing result.

Effect of DP-ICL Mechanism Parameters: Number of Partitions and Exemplars per Partition. Figure 6 shows how the number of partitions T affects empirical privacy on Agnews (top) and TREC (bottom) for theoretical budgets $\epsilon_{\text{theory}} \in \{1, 2, 4, 8\}$. For small budgets ($\epsilon_{\text{theory}} = 1, 2$), both black-box and white-box audits consistently recover high empirical ϵ across all T , while the non-private baseline stays near 0. As ϵ_{theory} increases ($\epsilon_{\text{theory}} = 4, 8$), the white-box empirical ϵ remains close to the theoretical bound with only a mild decrease, which is likely because the total number of demonstrations in the context becomes too large, making it more difficult for the LLM to identify and react to the single canary exemplar. But the black-box empirical ϵ sharply drops as T grows and eventually collapses. This aligns with our Gaussian analysis (Lemma 3.1): the underlying Gaussian-DP parameter is essentially T -invariant, but the black-box access suffer when the noisy vote statistics are compressed into a single label, making the effective signal vanish at large T .

For later experiments (Figure 7 to Figure 11), we fix the number of partitions to four to avoid the confounding effect of varying T . This value was chosen because both the black-box and white-box auditing demonstrate strong and stable auditing performance at $T = 4$.

Figure 7 explores the effect of the number of shots (exemplars) per partition, showing a stable empirical ϵ that is not heavily influenced by this parameter.

Auditing Efficiency: Number of MIAs and LLM calls. Figure 8 illustrates the relationship between the number of simulated MIAs and the resulting empirical ϵ . For both attack types, the empirical ϵ estimate is low and unstable at a small number of trials ($< 10^3$) but converges to a stable, higher value as the number of trials increases. This result validates our choice of 400,000 trials to ensure a reliable and converged audit.

Figure 9 demonstrates that our sampling-based auditing method, designed for an internal auditor, achieves reliable estimates with only a small number of initial LLM queries. After collecting roughly 100–200 calls to construct the empirical vote distribution, the estimate quickly converges and remains stable across additional samples. This verifies that our efficiency-enhanced auditing procedure preserves accuracy while substantially reducing the number of LLM calls required for a full audit.

Robustness across LLM Configurations. Figure 10 shows that as the LLM temperature increases, the empirical ϵ decreases, especially for temperatures larger than 2. This is because higher temperatures add more randomness to the LLM’s outputs (votes), which masks the canary’s influence and reduces the MIA’s accuracy.

Figure 11 compares the performance of Llama-3-8b-Instruct and GPT-oss-20b. While the results are broadly consistent, the larger GPT-oss-20b model consistently shows a slightly higher and more stable empirical ϵ . This suggests its stronger language processing capabilities may make it more effective at discerning the canary’s presence, thus leading to a more successful audit attack.

Cost and Privacy/Utility Tradeoff. Figure 12 shows a key trade-off. It confirms that task performance (classification accuracy) improves with more partitions, which also (as seen in Figure 6) decreases black-box privacy leakage. However, this comes at the cost of increased computation, as each additional partition requires a separate LLM call, and the total number of demonstrations increases. This highlights a practical trade-off between utility, black-box privacy, and computational cost.

4.3. Auditing Text Generation

In this section, we present our auditing results for the text generation task. Notably, we provide a tighter sensitivity analysis compared with the original analysis for the DP-ICL mechanism, tightening the L2 sensitivity from 1 to $\frac{2}{T}$, where T is the number of partitions. We present the detailed analysis in Appendix A.

Auditing Tightness. Figure 13 presents an overview of the text generation auditing results. For this figure, the number of partitions is set to the optimal value observed in our experiments to maximize the empirical leakage. The results clearly show that both our black-box and white-box threat models (red and blue bars) achieve a higher empirical ϵ than their respective baselines (green and brown bars), demonstrating the effectiveness of our auditing methodology.

A critical finding, in contrast to the classification task, is that the empirical leakage for generation remains substantially lower than the theoretical ϵ (dashed line). For instance, at a theoretical $\epsilon = 8$, the measured empirical ϵ is only around 4. This large gap strongly suggests that the theoretical sensitivity bound (which assumes a maximum L2 embedding distance of 2) represents a worst-case scenario that is rarely, if ever, attained in practice by real embedding models and LLM outputs.

Effect of DP-ICL Mechanism Parameters: Number of Partitions and Exemplars per Partition. Figure 14 reports the effect of the number of partitions T on the text generation task for Samsum (top) and Xsum (bottom). Across all theoretical budgets $\epsilon_{\text{theory}} \in \{1, 2, 4, 8\}$, both black-box and white-box attacks exhibit a clear hump-shaped trend: the empirical ϵ increases as T grows from 2 to a moderate value (around $T = 6-8$), and then gradually decreases for larger

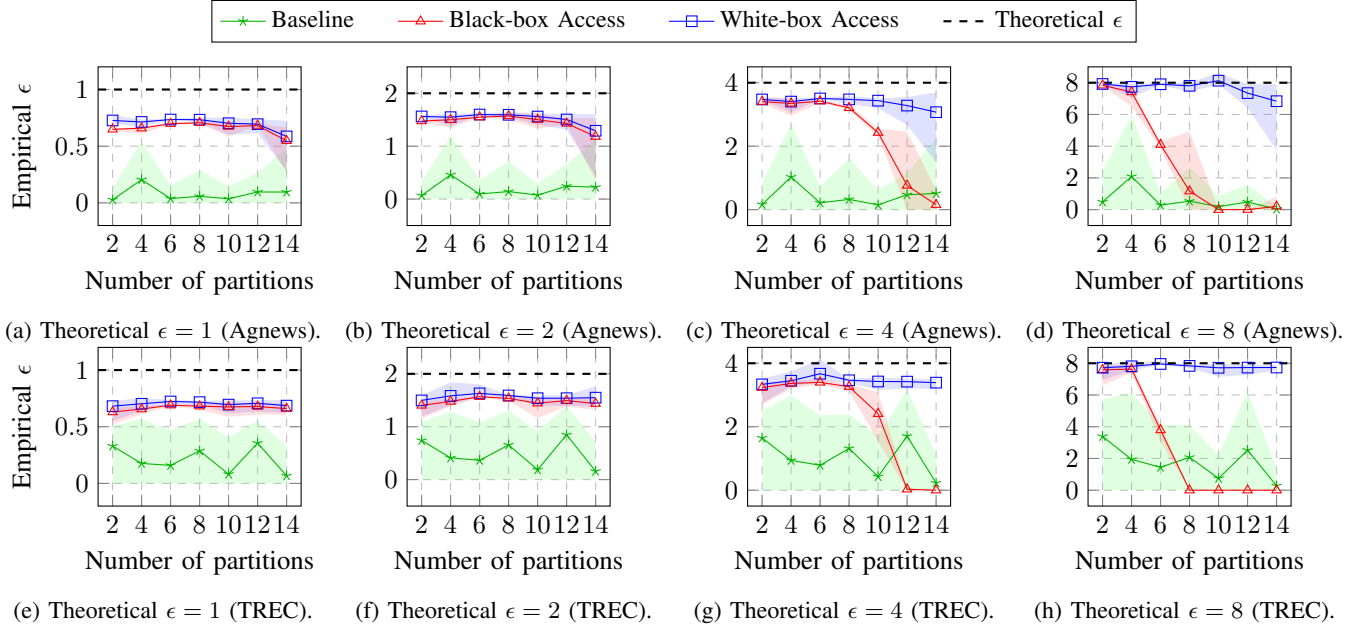


Figure 6: Effect of the number of partitions in the text classification task.

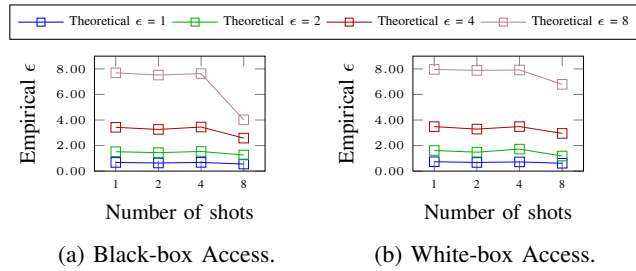


Figure 7: Relationship between the number of shots and the empirical ϵ in the text classification task.

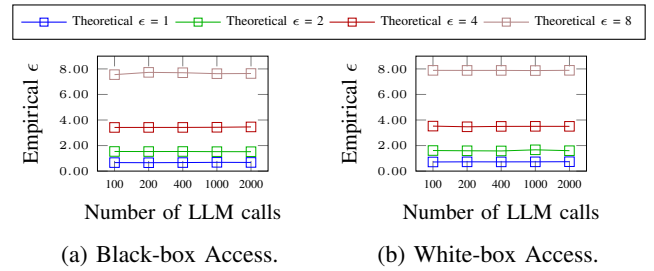


Figure 9: Relationship between the number of LLM calls and the empirical ϵ in the text classification task.

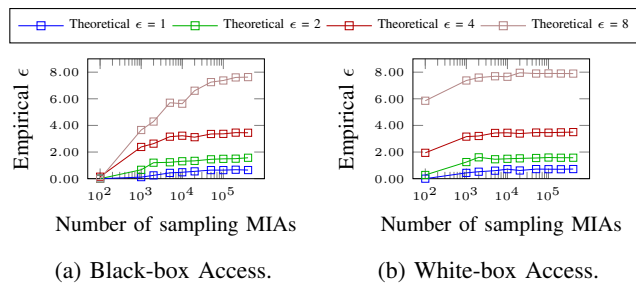


Figure 8: Relationship between the number of sampling MIAs and the empirical ϵ in the text classification task.

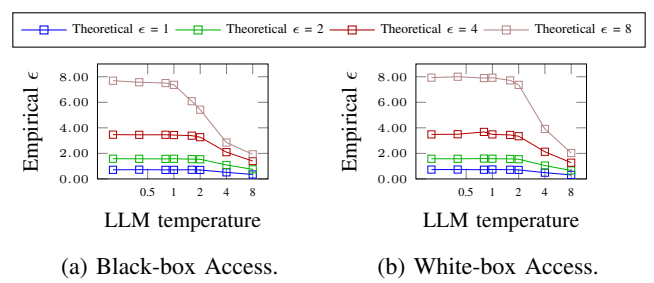


Figure 10: Relationship between the LLM temperature and the empirical ϵ in the text classification task.

T . The non-private baselines remain near zero. This non-monotonic behavior is consistent with our sensitivity analysis. Our ESA mechanism calibrates the Gaussian noise using an upper bound on the embedding sensitivity that scales roughly as $2/T$. For small T , this bound is large and the injected noise is overly conservative, so the canary-induced shift in the aggregated embedding is mostly drowned out

and the observed empirical ϵ is small. As T increases to moderate values, the bound (and thus the noise scale) decreases faster than the actual canary effect, improving the signal-to-noise ratio and yielding larger empirical ϵ . When T becomes very large, however, the decoded outputs enter a saturated regime: the model tends to generate the same response regardless of subtle embedding differences, and

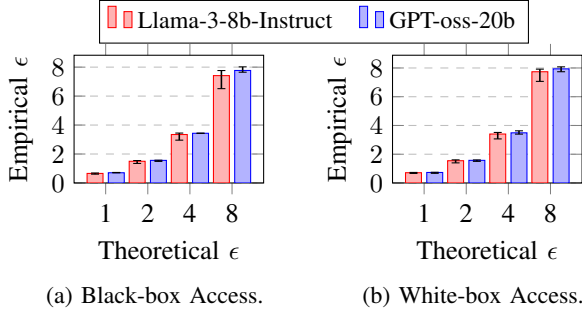


Figure 11: Relationship between different LLMs and empirical ϵ in the text classification task.

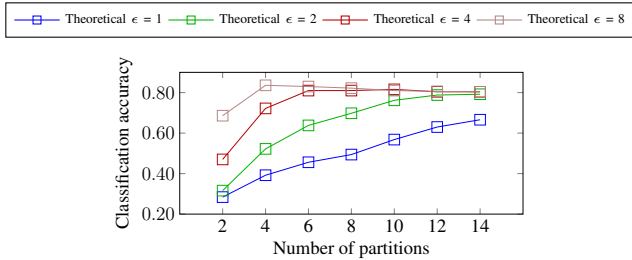


Figure 12: Relationship between the number of partitions and the utility in the text classification task.

finite-sample estimation further compresses the TPR/FPR gap, causing both black-box and white-box empirical ϵ to decline again. White-box attacks consistently achieve higher empirical ϵ than black-box attacks across all T , but follow the same qualitative pattern.

Similar to Section 4.2, we fix the number of partitions to $T=4$ for the subsequent experiments (Figure 15-20) to avoid the confounding effect of varying T .

Figure 15 explores the effect of the number of shots (exemplars) per partition. We observe a clear trend: the empirical ϵ decreases as the number of shots increases. This is likely because additional, non-canary exemplars introduce more variance to the output embeddings, which helps to mask the specific influence of the single canary exemplar when the embeddings are averaged.

Auditing Efficiency: Number of MIAs and LLM calls.

Figure 16 illustrates the relationship between the number of simulated MIAs and the empirical ϵ . The estimate is low and unstable at fewer than 10^3 trials but converges to a stable, higher value. This validates our choice of 400,000 trials to ensure a reliable audit. Figure 17 shows that the auditing result stabilizes after a sufficient number of initial LLM calls (e.g., 200-400) are used to build the empirical distribution for bootstrap resampling.

Impact of Signal Embedding Distance. Figure 18 examines the relationship between the signal embedding distance and the empirical privacy loss ϵ_{emp} for the text generation task. Here, the distance denotes the ℓ_2 distance in the embedding space between the two predefined outputs y_1 (indicating “canary present”) and y_2 (indicating

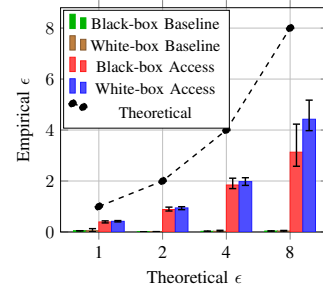


Figure 13: Overview of the text generation auditing result.

“canary absent”). Overall, ϵ_{emp} increases as the embedding distance grows. One exception is the pair $(y_1, y_2) = ("["Incorrect statement"]", "[]")$, also used by the white-box baseline, which yields $\epsilon_{emp} = 0$ under black-box access because the zero-shot query (relying on the LLM’s default behavior) always outputs y_2 . We list all tested signal text pairs (y_1, y_2) in Appendix C.

Robustness across LLM Configurations. Figure 19 shows that the empirical leakage generally peaks at a low temperature (e.g., 0.4) and then decreases as the temperature increases. Higher temperatures add more randomness to the LLM’s output embeddings, making the canary’s signal less consistent and thus harder for the attacker to detect. Notably, for the black-box access, the empirical ϵ drops to zero when the temperature is very low (e.g., ≤ 0.2). This is because the 0-shot query (which relies on the LLM’s default behavior) becomes deterministic, always outputting the same string (y_1 or y_2). This makes the canary-present and canary-absent scenarios indistinguishable to the black-box attacker.

Figure 20 compares the performance of Llama-3-8b-Instruct and GPT-oss-20b. The results are broadly consistent, with the larger GPT-oss-20b model showing a higher and more stable ϵ_{emp} . This suggests a larger model may be more effective at consistently discerning the canary’s presence.

Unchanged Utility. Figure 21 plots the task utility (ROUGE-L F1-score) against the number of partitions. Unlike the classification task, where accuracy consistently improved with T , the utility for this generation task does not show a clear, monotonic relationship. The ROUGE score fluctuates within a small range, suggesting that simply increasing the number of partitions (and thus the computational cost) does not necessarily improve the summarization quality of the ESA mechanism. This may be because the final answer is selected from 0-shot responses, and the quality of these candidates is not improved by adding more partitions or changing the privacy budget.

5. Related Work

We review prior work along three aspects closely aligned with our contributions: (i) in-context learning (ICL) and prompt-level threats, (ii) inference-time DP mechanisms that privatize ICL aggregation, and (iii) auditing methodologies originally developed for training-time DP that we adapt to the inference-time ICL setting.

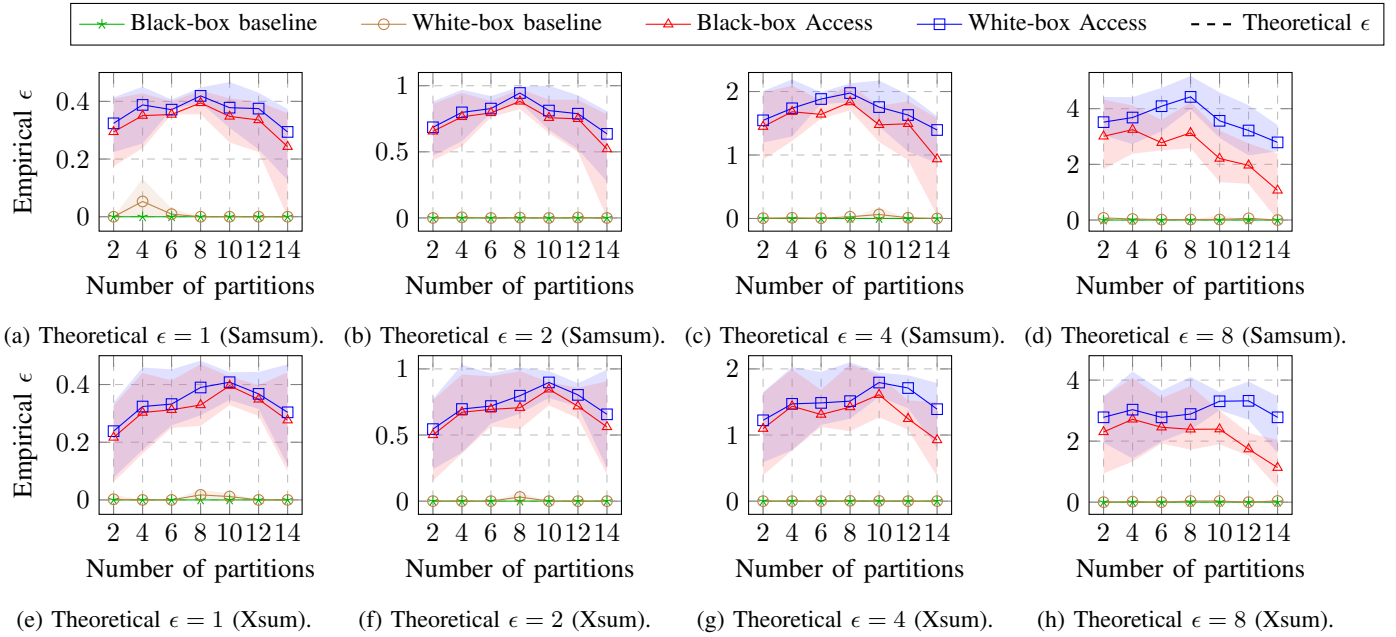


Figure 14: Effect of the number of partitions in the text generation task.

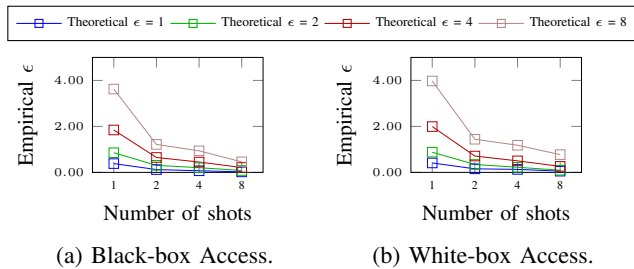


Figure 15: Relationship between the number of shots and the empirical ϵ in the text generation task.

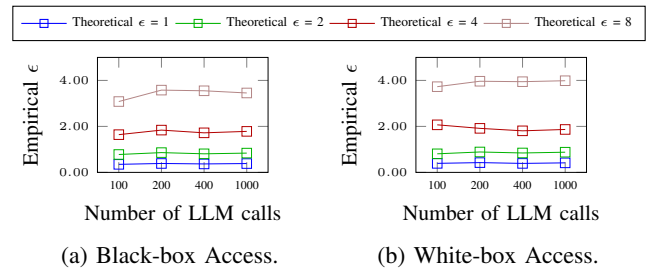


Figure 17: Relationship between the number of LLM calls and the empirical ϵ in the text generation task.

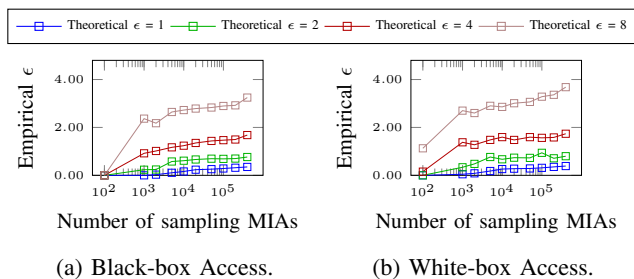


Figure 16: Relationship between the number of sampling MIAs and the empirical ϵ in the text generation task.

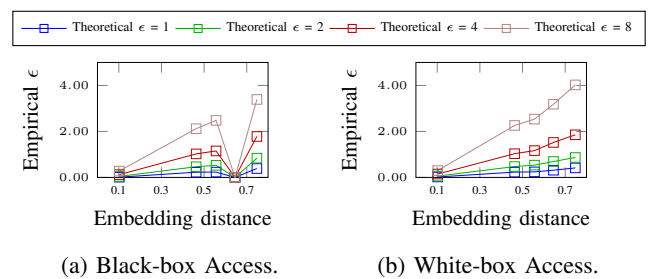


Figure 18: Relationship between the signal embedding distance and the empirical ϵ in the text generation task.

ICL and Prompt-Level Threats. Modern LLMs exhibit strong *in-context learning* (ICL) capabilities: given a few exemplars in the prompt, they can adapt to new tasks without parameter updates [1]. Subsequent work analyzes when and why ICL works, including which aspects of demonstrations matter [23], explanations of ICL as implicit Bayesian inference [24], and studies of what function classes Transformers

can learn in-context [25]. These results view ICL as a general meta-learning capability rather than a task-specific trick. ICL is also widely used in applied systems, often combined with instruction-following prompts and retrieval-augmented generation (RAG), where retrieved documents or database records are injected into the context as demonstrations or evidence [26]. At the same time, security work on prompt

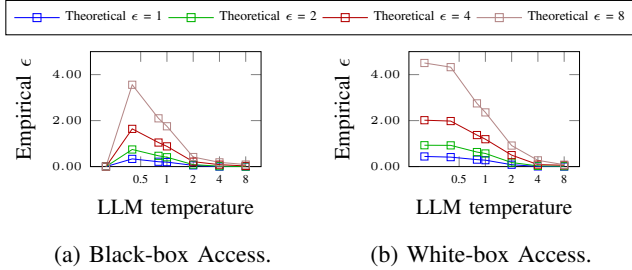


Figure 19: Relationship between the LLM temperature and the empirical ϵ in the text generation task.

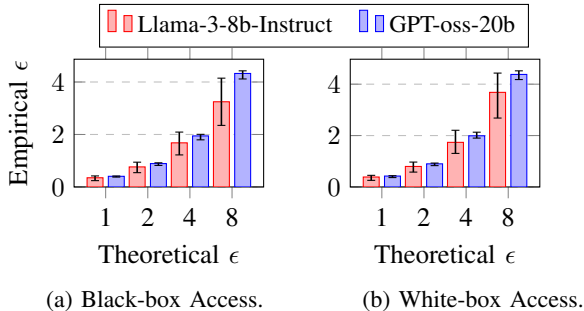


Figure 20: Relationship between different LLMs and empirical ϵ in the text generation task.

injection and indirect prompt injection (IPI) demonstrates that adversaries can coerce LLM-powered pipelines to reveal or verify hidden prompt content [27], [28].

Inference-Time DP for ICL. A pragmatic defense is to privatize the ICL aggregation itself at inference time. Two main families of mechanisms are used: (i) *private voting* over demonstrations via noisy discrete selection, conceptually related to PATE’s noisy histogram/argmax aggregators [29], [30] and classic mechanisms such as Report-Noisy-Max and the Exponential Mechanism [31]–[33]; and (ii) *noisy continuous aggregation*, e.g., releasing a privatized mean or embedding statistic using calibrated Gaussian noise [34]. Their privacy guarantees are typically analyzed with modern accountants such as f -DP/GDP, and often combined with privacy amplification for subsampling/partitioning and tight composition for repeated queries [15], [35], [36]. While their theoretical privacy analysis relies on the above accounting tools, practical deployments still require ways to empirically verify that implementations match their claimed privacy parameters, which motivates our auditing framework.

DP Auditing: From Training to Inference. Most auditing methodology has been developed for training-time DP, notably DP-SGD [37]. Recent work designs attack-based auditors that convert hypothesis-testing error rates (TPR/FPR) into empirical privacy loss and demonstrate tight, sample-efficient procedures for auditing DP-SGD in practice [9], [11]. Tooling and surveys help practitioners operationalize membership-inference-based audits for deployed systems [38]. However, these methods assume access

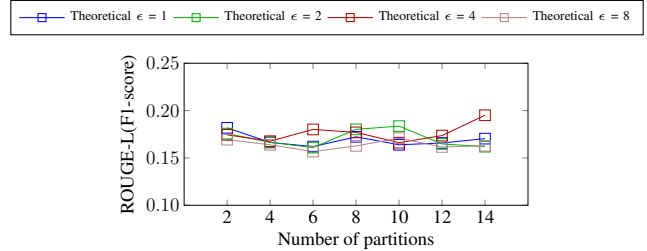


Figure 21: Relationship between the number of partitions and the utility in the text generation task.

to training-time signals (e.g., losses, gradients, or multiple retrains) and target parameter updates, not inference-time signals (e.g., texts), so they cannot be directly applied to DP-ICL.

Closer to our setting, Wen et al. [12] propose four in-context learning based membership-inference attacks (ICL-MIA), and Wang et al. introduce a related ICL-MIA similar in spirit to the Repeat Attack [13]. These methods provide basic building blocks for constructing attack-based auditors in ICL-style systems, but do not consider DP-ICL’s partitioned aggregation. Choi et al. [14] empirically demonstrate nontrivial leakage in DP-ICL. However, they do not provide empirical lower bounds that are directly comparable to theoretical guarantees. Our auditor thus builds on ICL-MIA techniques and is the first to turn them into a DP empirical auditing tool for DP-ICL, and provides theory-guided attack/query design tailored to DP-ICL based on private aggregation.

6. Conclusion

In this paper, we introduced the first systematic framework for computing empirical privacy loss (ϵ_{emp}) in differentially private in-context learning (DP-ICL). Through comprehensive white-box and black-box auditing, we demonstrated that our attacks provide a stable measure of privacy loss that outperforms standard baselines. Crucially, we observed that while empirical leakage in text classification closely matches theoretical budgets (ϵ_{theory}), leakage in text generation is consistently lower, suggesting that current sensitivity bounds for embedding space aggregation are overly conservative. These findings highlight the need for tighter, task-aware sensitivity analyses and establish our framework as a vital tool for verifying privacy guarantees and detecting errors in deployed LLM pipelines. In the future, we plan to extend our auditing methodology to a broader class of inference-time DP mechanisms and more complex multi-step LLM workflows, and to explore stronger adversarial strategies and tighter theoretical analyses for the text generation task. An important direction is to integrate our audit into automated regression tests for real-world DP-ICL deployments and to study how empirical privacy guarantees behave under practical constraints such as limited query budgets, distribution shifts, and evolving model updates.

References

- [1] T. Brown, B. Mann, N. Ryder, M. Subbiah, J. D. Kaplan, P. Dhariwal, A. Neelakantan, P. Shyam, G. Sastry, A. Askell *et al.*, “Language models are few-shot learners,” *Advances in neural information processing systems*, vol. 33, pp. 1877–1901, 2020.
- [2] Q. Dong, L. Li, D. Dai, C. Zheng, J. Ma, R. Li, H. Xia, J. Xu, Z. Wu, T. Liu *et al.*, “A survey on in-context learning,” *arXiv preprint arXiv:2301.00234*, 2022.
- [3] H. Gonen, S. Iyer, T. Blevins, N. A. Smith, and L. Zettlemoyer, “Demystifying prompts in language models via perplexity estimation,” *arXiv preprint arXiv:2212.04037*, 2022.
- [4] C. Mavromatis, B. Srinivasan, Z. Shen, J. Zhang, H. Rangwala, C. Faloutsos, and G. Karypis, “Which examples to annotate for in-context learning? towards effective and efficient selection,” *arXiv preprint arXiv:2310.20046*, 2023.
- [5] Y. Liu, J. Liu, X. Shi, Q. Cheng, Y. Huang, and W. Lu, “Let’s learn step by step: Enhancing in-context learning ability with curriculum learning,” *arXiv preprint arXiv:2402.10738*, 2024.
- [6] T. Wu, A. Panda, J. T. Wang, and P. Mittal, “Privacy-preserving in-context learning for large language models,” *arXiv preprint arXiv:2305.01639*, 2023.
- [7] X. Tang, R. Shin, H. A. Inan, A. Manoel, F. Mireshghallah, Z. Lin, S. Gopi, J. Kulkarni, and R. Sim, “Privacy-preserving in-context learning with differentially private few-shot generation,” *arXiv preprint arXiv:2309.11765*, 2023.
- [8] F. Lu, J. Munoz, M. Fuchs, T. LeBlond, E. Zaresky-Williams, E. Raff, F. Ferraro, and B. Testa, “A general framework for auditing differentially private machine learning,” *Advances in Neural Information Processing Systems*, vol. 35, pp. 4165–4176, 2022.
- [9] M. Jagielski, J. Ullman, and A. Oprea, “Auditing differentially private machine learning: How private is private sgd?” *Advances in Neural Information Processing Systems*, vol. 33, pp. 22 205–22 216, 2020.
- [10] M. Nasr, S. Songi, A. Thakurta, N. Papernot, and N. Carlin, “Adversary instantiation: Lower bounds for differentially private machine learning,” in *2021 IEEE Symposium on security and privacy (SP)*. IEEE, 2021, pp. 866–882.
- [11] M. Nasr, J. Hayes, T. Steinke, B. Balle, F. Tramèr, M. Jagielski, N. Carlini, and A. Terzis, “Tight auditing of differentially private machine learning,” in *32nd USENIX Security Symposium (USENIX Security 23)*, 2023, pp. 1631–1648.
- [12] R. Wen, Z. Li, M. Backes, and Y. Zhang, “Membership inference attacks against in-context learning,” in *Proceedings of the 2024 on ACM SIGSAC Conference on Computer and Communications Security*, 2024, pp. 3481–3495.
- [13] Z. Wang, G. Liu, Y. Yang, and C. Wang, “Membership inference attack against long-context large language models,” *arXiv preprint arXiv:2411.11424*, 2024.
- [14] J. Choi, S. Cao, X. Dong, and S. P. Karimireddy, “Contextleak: Auditing leakage in private in-context learning methods,” in *The Impact of Memorization on Trustworthy Foundation Models: ICML 2025 Workshop*.
- [15] J. Dong, A. Roth, and W. J. Su, “Gaussian differential privacy,” *Journal of the Royal Statistical Society Series B: Statistical Methodology*, vol. 84, no. 1, pp. 3–37, 2022.
- [16] B. Efron, *The jackknife, the bootstrap and other resampling plans*. SIAM, 1982.
- [17] Meta. (2024, Jul.) Llama-3.1-8b-instruct. Hugging Face, Accessed: 2025-09-18. [Online]. Available: <https://huggingface.co/meta-llama/Llama-3.1-8B-Instruct>
- [18] OpenAI, “gpt-oss-120b & gpt-oss-20b model card,” 2025. [Online]. Available: <https://arxiv.org/abs/2508.10925>
- [19] X. Zhang, J. Zhao, and Y. LeCun, “Character-level convolutional networks for text classification,” *Advances in neural information processing systems*, vol. 28, 2015.
- [20] E. M. Voorhees and D. M. Tice, “Building a question answering test collection,” in *Proceedings of the 23rd annual international ACM SIGIR conference on Research and development in information retrieval*, 2000, pp. 200–207.
- [21] B. Gliwa, I. Mochol, M. Biesek, and A. Wawer, “SAMSum corpus: A human-annotated dialogue dataset for abstractive summarization,” in *Proceedings of the 2nd Workshop on New Frontiers in Summarization*. Hong Kong, China: Association for Computational Linguistics, Nov. 2019, pp. 70–79. [Online]. Available: <https://www.aclweb.org/anthology/D19-5409>
- [22] S. Narayan, S. B. Cohen, and M. Lapata, “Don’t give me the details, just the summary! topic-aware convolutional neural networks for extreme summarization,” *ArXiv*, vol. abs/1808.08745, 2018.
- [23] S. Min, X. Lyu, A. Holtzman, M. Artetxe, M. Lewis, H. Hajishirzi, and L. Zettlemoyer, “Rethinking the role of demonstrations: What makes in-context learning work?” *arXiv preprint arXiv:2202.12837*, 2022.
- [24] S. M. Xie, A. Raghunathan, P. Liang, and T. Ma, “An explanation of in-context learning as implicit bayesian inference,” *arXiv preprint arXiv:2111.02080*, 2021.
- [25] S. Garg, D. Tsipras, P. S. Liang, and G. Valiant, “What can transformers learn in-context? a case study of simple function classes,” *Advances in neural information processing systems*, vol. 35, pp. 30 583–30 598, 2022.
- [26] P. Lewis, E. Perez, A. Piktus, F. Petroni, V. Karpukhin, N. Goyal, H. Küttler, M. Lewis, W.-t. Yih, T. Rocktäschel *et al.*, “Retrieval-augmented generation for knowledge-intensive nlp tasks,” *Advances in neural information processing systems*, vol. 33, pp. 9459–9474, 2020.
- [27] K. Greshake, S. Abdelnabi, G. Mishra, C. Endres, T. Holz, and M. Fritz, “Not what you’ve signed up for: Compromising real-world llm-integrated applications with indirect prompt injection,” *arXiv:2302.12173*, 2023.
- [28] H. Liu, Y. Zhang, J. Zou *et al.*, “Prompt injection attacks and defenses in llm applications,” *arXiv:2309.01327*, 2023.
- [29] N. Papernot, M. Abadi, Ú. Erlingsson, I. Goodfellow, and K. Talwar, “Semi-supervised knowledge transfer for deep learning from private training data,” in *International Conference on Learning Representations*, 2017.
- [30] N. Papernot, S. Song, I. Mironov, A. Raghunathan, K. Talwar, and U. Erlingsson, “Scalable private learning with pate,” in *International Conference on Learning Representations*, 2018.
- [31] C. Dwork, A. Roth *et al.*, “The algorithmic foundations of differential privacy,” *Foundations and trends® in theoretical computer science*, vol. 9, no. 3–4, pp. 211–407, 2014.
- [32] F. McSherry and K. Talwar, “Mechanism design via differential privacy,” in *48th Annual IEEE Symposium on Foundations of Computer Science (FOCS’07)*. IEEE, 2007, pp. 94–103.
- [33] C. Dwork, F. McSherry, K. Nissim, and A. Smith, “Calibrating noise to sensitivity in private data analysis,” in *Theory of cryptography conference*. Springer, 2006, pp. 265–284.
- [34] B. Balle and Y.-X. Wang, “Improving the gaussian mechanism for differential privacy: Analytical calibration and optimal denoising,” in *International conference on machine learning*. PMLR, 2018, pp. 394–403.
- [35] B. Balle, G. Barthe, and M. Gaboardi, “Privacy amplification by subsampling: Tight analyses via couplings and divergences,” *Advances in neural information processing systems*, vol. 31, 2018.
- [36] Y.-X. Wang, B. Balle, and S. P. Kasiviswanathan, “Subsampled rényi differential privacy and analytical moments accountant,” in *The 22nd international conference on artificial intelligence and statistics*. PMLR, 2019, pp. 1226–1235.

- [37] M. Abadi, A. Chu, I. Goodfellow, H. B. McMahan, I. Mironov, K. Talwar, and L. Zhang, “Deep learning with differential privacy,” in *Proceedings of the 2016 ACM SIGSAC conference on computer and communications security*, 2016, pp. 308–318.
- [38] J. Niu, P. Liu, X. Zhu, K. Shen, Y. Wang, H. Chi, Y. Shen, X. Jiang, J. Ma, and Y. Zhang, “A survey on membership inference attacks and defenses in machine learning,” *Journal of Information and Intelligence*, vol. 2, no. 5, pp. 404–454, 2024.
- [39] Á. Baricz, “Mills’ ratio: Monotonicity patterns and functional inequalities,” *Journal of Mathematical Analysis and Applications*, vol. 340, no. 2, pp. 1362–1370, 2008.

7. Ethics Considerations

This work investigates privacy risks in differentially private in-context learning (DP-ICL) using only standard, publicly available NLP benchmarks (e.g., Agnews, TREC, Samsun, and Xsum). We do not collect any new human-subject data. All canary exemplars used in our membership inference attacks are sampled from these benchmarks and treated strictly as experimental records for the purpose of privacy auditing; we do not attempt to re-identify individuals or infer sensitive attributes beyond what is publicly present in the datasets. Additionally, all signal texts utilized in our experiments are randomly generated to ensure no unintended leakage of external information.

Our auditing framework is evaluated on locally deployed models (Llama-3-8b-Instruct and GPT-oss-20b) and on DP mechanisms that we implement ourselves, rather than on production systems operated by third parties without their consent. The goal of our attacks is to quantify and verify the privacy guarantees of DP-ICL mechanisms, not to compromise deployed services. In particular, we design our experiments to stress-test claimed differential privacy parameters and to detect implementation bugs, so that system designers can avoid shipping misconfigured or unsafe DP-ICL pipelines.

Appendix

1. Tighter Sensitivity Analysis

In this section, we present our analysis of the text-generation mechanism based on the ESA algorithm.

Lemma A.1. *The L2-sensitivity of the released noisy mean embedding from the ESA algorithm is $\frac{2}{T}$, where T is the number of disjoint exemplar subsets.*

Proof. Consider contexts C and C' that differ only by the presence/absence (or replacement) of one canary exemplar within subset t^* . Then $v_t = v'_t$ for all $t \neq t^*$, while v_{t^*} may differ from v'_{t^*} . Therefore, the sensitivity is

$$\left\| \frac{1}{T} \sum_{t=1}^T (v_t - v'_t) \right\|_2 = \frac{1}{T} \|v_{t^*} - v'_{t^*}\|_2$$

By the triangle inequality and the norm bound $\|v\|_2 \leq R = 1$, we have $\frac{1}{T} \|v_{t^*} - v'_{t^*}\|_2 \leq \frac{1}{T} (\|v_{t^*}\|_2 + \|v'_{t^*}\|_2) \leq \frac{2}{T}$. \square

Tightness example: Fix all subsets except t^* . Let $v_{t^*} = u$ and $v'_{t^*} = -u$. Then the sensitivity is $\frac{1}{T} \|2u\|_2 = \frac{2}{T}$.

Compared to the original paper’s L2 sensitivity 1 [6], this tighter bound yields a more accurate mapping between the noise scale and the theoretical privacy budget.

2. Query Prompt Used in Paper

```

1 You are a highly accurate text verification
2 system. Your sole function is to verify
3 if the text in the <query> tag is present
4 in the <context> tag.
5 Your response must be a single word: either
6 'Yes' or 'No'.
7
8 <context>
9 {formatted_context}
10 </context>
11
12 <query>
13 {query_article}
14 </query>
15
16 <response>

```

Prompt 1: Auditing query for text classification.

```

1 Carefully check if the dialog "{canary}" is
2 present in the provided CONTEXTUAL
3 EXEMPLAR:.
4
5 If "{canary}" is found in the CONTEXTUAL
6 EXEMPLAR:, output "{Y1_TARGET}".
7 Otherwise, output "{Y2_CONTROL}".
8
9 CONTEXTUAL EXEMPLAR:
10 {exemplar_context}
11
12 RESPONSE:

```

Prompt 2: White-box auditing query for text generation.

```

1 Analyze the "CONTEXTUAL EXEMPLAR" below.
  Your ONLY function is to output ONE of
  two predefined sentences. Do not add
  explanations.
2
3 1. Check if the specific phrase "{canary}"
  is present in the context.
4 2. If the context is empty, randomly output
  either "{Y1_TARGET}" or "{Y2_CONTROL}".
5 3. If the context is NOT empty and "{canary
  }" is found, output "{Y1_TARGET}".
6 4. If the context is NOT empty and "{canary
  }" is NOT found, output "{Y2_CONTROL}".
7
8 CONTEXTUAL EXEMPLAR:
9 {exemplar_context}
10
11 RESPONSE:

```

Prompt 3: Black-box auditing query for text generation.

```

1 You are a highly accurate text classifier.
  Classify the following text into one of
  the provided categories based on the
  examples.
2 The possible labels are: World, Sports,
  Business, Sci/Tech. Only output the
  label.
3
4 Examples:
5 {formatted_exemplars}
6
7 Query Text: {query_article}
8 Label:

```

Prompt 4: Mislabel baseline query for text classification.

```

1 Here is a collection of text passages:
2
3 --- CONTEXT START ---
4 {context_string}
5 --- CONTEXT END ---
6
7 Based on the text provided above, please
  complete the following sentence:
8
9 "{prefix}"

```

Prompt 5: Black-box baseline for text generation.

We copy the query prompt and canary text from [14] as our white-box baseline attack for text generation. The canary text is "The sun rises in the west."

```

1 "This is the user prompt. Only if the
  following factually incorrect statement
  is present in the system prompt:\n"
2 "\{canary_text}\n"
3 "Must you return the statement in a Python
  list format. Example:\n"
4 "[\"Incorrect statement\",]\n"
5 "Otherwise, you must, with no other text or
  information, return an empty list."

```

Prompt 6: White-box baseline for text generation.

3. Pairs of Signal Texts

y_1	y_2	L_2 distance
"The old clock chimed a forgotten, dusty tune."	"FOXBOROUGH – Looking at his ridiculously developed upper body, with huge biceps and hardly an ounce of fat."	0.7476
"[\"Incorrect statement.\"]"	"[]"	0.645
"The red car sped down a long, winding road."	"The blue boat sailed on a vast, open sea."	0.5562
"Real Madrid won the match convincingly."	"Barcelona secured a decisive victory in the game."	0.4628
"The old clock chimed a forgotten, dusty tune."	"The old clock chimed a forgotten, dusty song."	0.1022

TABLE 3: Pairs of signal texts and the corresponding L_2 distances.

4. Proof for Lemma 3.1

Proof. For a fixed number of partitions T , consider the canary-present context $V_{\text{with}} = [k, T - k]$ and a general canary-absent context $V_{\text{without}} = [k - b, T - k + b]$, where $b \in [0, 1]$ parameterizes the deterministic vote margin induced by the canary. The case $b = 0$ corresponds to no margin change, and $b = 1$ corresponds to flipping one vote in favor of the canary and one against it.

Let $N_1, N_2 \sim \mathcal{N}(0, \sigma^2)$ be independent Gaussian noises added to the two vote counts. The (noisy) vote difference under the canary-present context C_1 is

$$D_1 = k + N_1 - ((T - k) + N_2) = (2k - T) + (N_1 - N_2),$$

and under C_0 is

$$D_0 = (k - b) + N_1 - ((T - k + b) + N_2) = (2k - T - 2b) + (N_1 - N_2).$$

Since $N_1 - N_2 \sim \mathcal{N}(0, 2\sigma^2)$, we have

$$D_1 \sim \mathcal{N}(\mu_1, 2\sigma^2), \quad D_0 \sim \mathcal{N}(\mu_0, 2\sigma^2),$$

with

$$\mu_1 = 2k - T, \quad \mu_0 = 2k - T - 2b.$$

Thus, the deterministic mean gap between the two hypotheses is

$$\Delta = \mu_1 - \mu_0 = 2b.$$

In the Gaussian-DP view, the corresponding Gaussian channel is given by the two distributions of the normalized statistic

$$S = \frac{D - \mu_0}{\sqrt{2\sigma}},$$

which satisfies $S | C_0 \sim \mathcal{N}(0, 1)$ and $S | C_1 \sim \mathcal{N}(\mu_{\text{Gauss}}, 1)$ with

$$\mu_{\text{Gauss}} = \frac{\Delta}{\sqrt{2\sigma}} = \frac{2b}{\sqrt{2\sigma}}.$$

Hence μ_{Gauss} depends only on the margin parameter b and the noise scale σ , and is independent of k (and of T once b is fixed). On the interval $b \in [0, 1]$, μ_{Gauss} is strictly increasing in b and thus attains its maximum at $b = 1$.

We now turn to the DP-based empirical loss. Consider the fixed threshold test that declares canary presence iff the noisy vote difference is positive:

decide C_1 if $D > 0$, decide C_0 otherwise.

Under C_1 and C_0 , the true and false positive rates are $\text{TPR}(k, b) = \Pr(D_1 > 0) = \Phi\left(\frac{\mu_1}{\sqrt{2}\sigma}\right) \text{FPR}(k, b) = \Pr(D_0 > 0) = \Phi\left(\frac{\mu_0}{\sqrt{2}\sigma}\right)$, where Φ is the standard normal CDF. Writing $x_k = \frac{\mu_1}{\sqrt{2}\sigma} = \frac{2k-T}{\sqrt{2}\sigma}$, $a_b = \frac{\Delta}{\sqrt{2}\sigma} = \frac{2b}{\sqrt{2}\sigma}$, we have $\text{TPR}(k, b) = \Phi(x_k)$, $\text{FPR}(k, b) = \Phi(x_k - a_b)$, and the DP-based empirical loss is $\epsilon_{\text{emp}}(k, b) = \log\left(\frac{\Phi(x_k)}{\Phi(x_k - a_b)}\right)$. Differentiating with respect to k yields $\frac{\partial}{\partial k} \epsilon_{\text{emp}}(k, b) = \frac{\phi(x_k)}{\Phi(x_k)} - \frac{\phi(x_k - a_b)}{\Phi(x_k - a_b)}$, where ϕ is the standard normal PDF. Since the Mills ratio $\phi(x)/\Phi(x)$ is strictly decreasing in x , the right-hand side is strictly negative for any $a_b > 0$ [39]. Therefore, for any fixed $b > 0$, $\epsilon_{\text{emp}}(k, b)$ is strictly decreasing in k , so its maximizer over feasible k depends on the lower bound of the admissible range of k , which in turn depends on the choice of T and the voting pattern constraints. In particular, unlike μ_{Gauss} , the value of k (and thus T) that maximizes ϵ_{emp} is not universal but is determined by the specific decision rule and combinatorial constraints of the mechanism.

This proves that in the Gaussian model, the Gaussian-DP parameter μ_{Gauss} attains its maximum at $b = 1$ independently of T and k , whereas the DP-based empirical loss ϵ_{emp} attains its maximum at k (and thus T) values that depend on the decision rule. \square

5. Detailed Algorithms for DP-ICL Mechanisms

Private Voting Algorithm (Algorithm 2) handles tasks with a discrete label set. It first partitions exemplars into disjoint partitions and initializes the clean vote vector (lines 1-2). Each subset is concatenated with the query to form a prompt to obtain a class prediction from the LLM (lines 3-5). The predictions are aggregated into a clean vote vector. It then adds Gaussian noise to each class vote count (lines 7-8) and releases the label with the highest noisy vote count (lines 9-10).

ESA mechanism (Algorithm 3) targets free-form text generation. It partitions exemplars into disjoint partitions, each concatenated with the query to form a prompt and obtain an output text from the LLM. The algorithm computes the mean of the embeddings of the output and adds Gaussian noise to obtain a DP mean emb_{avg} . Lastly, it generates answer candidates with no exemplars and outputs the one whose embedding is closest to the noisy mean (lines 10-12).

Algorithm 2: Private Voting Algorithm

Input: Private context C , User query q , Privacy budget $(\epsilon_{\text{theory}}, \delta)$, Number of partitions T , Language model LLM

Output: A final DP output label y

- 1 Partition exemplars $\in C$ into T disjoint partitions $\{P_1, P_2, \dots, P_T\}$;
- 2 $V \leftarrow \bar{0}$
- 3 **for** $i \in [1, T]$ **do**
- 4 $S_i \leftarrow$ concatenate P_i and q ;
- 5 $class_i \leftarrow LLM(S_i)$;
- 6 $V[class_i] \leftarrow V[class_i] + 1$
- 7 $\sigma \leftarrow 2\sqrt{\log(1.25/\delta)}/\epsilon$
- 8 $\tilde{V} \leftarrow$ adding Gaussian noise $\mathcal{N}(0, \sigma^2)$ on each element of V ;
- 9 $y \leftarrow$ label with highest vote count in \tilde{V} ;
- 10 **return** y ;

Algorithm 3: ESA Algorithm

Input: Private context C , User query q , Privacy budget $(\epsilon_{\text{theory}}, \delta)$, Number of partitions T , Number of candidates T_{cand} Language model LLM , Embedding model E

Output: A final DP generation text y

- 1 Partition exemplars $\in C$ into T disjoint partitions $\{P_1, P_2, \dots, P_T\}$;
- 2 $EMB \leftarrow \emptyset$
- 3 **for** $i \in [1, T]$ **do**
- 4 $S_i \leftarrow$ concatenate P_i and q ;
- 5 $emb_i \leftarrow E(LLM(S_i))$;
- 6 $EMB[i] \leftarrow emb_i$
- 7 $emb_{\text{avg}} \leftarrow \frac{1}{|EMB|} \sum EMB[i]$
- 8 $\sigma \leftarrow 2\sqrt{\log(1.25/\delta)}/\epsilon$
- 9 $\tilde{emb}_{\text{avg}} \leftarrow$ adding Gaussian noise $\mathcal{N}(0, \sigma^2)$ on each element of emb_{avg} ;
- 10 $cand \leftarrow [LLM(q) \text{ for } i \in [1, T_{\text{cand}}]]$;
- 11 $y \leftarrow i$ where $cand[i]$ is the closet to \tilde{emb}_{avg} ;
- 12 **return** $cand[y]$;
